BWIP SITE TECHNICAL POSITION INTERPRETATION OF HYDROGEOLOGIC TEST IN DEEP BOREHOLES USING DATA OBTAINED BY UPHOLE MEASUREMENTS

GOLDER ASSOCIATES

AUGUST, 1984

TABLE OF CONTENTS

APPENDIX A - ESTIMATION OF FRICTIONAL LOSSES IN DOWNHOLE EQUIPMENT

TABLES

FIGURES

823-1033/RPT/OVERSHOOT/FNT PGS

1.0 BACKGROUND

1.1 PURPOSE

Performance assessment of a repository in basalt will require evaluation of the direction and magnitude of groundwater flow from the repository to the accessible environment during both the pre-emplacement and post-closure time periods. Knowledge of the hydraulic properties (e.g., hydraulic conductivity, effective porosity) of the rock media and the driving gradients causing groundwater flow will be needed for this assessment. In general, hydraulic properties and gradients are inferred from data obtained in hydrogeologic tests and monitoring installations in boreholes. These tests rely upon accurate measurement of formation pressure or head, and flow rate within the test zone.

Measurement of head and flow rate by uphole methods is accepted as the industry standard for water supply hydrology, and is, in general, both accurate and cost effective for this technical application. In the case of testing in deep boreholes at Hanford, the test interval is some 1000 meters from the surface, and the conditions of water at this depth differ considerably from that of a sample of the same water under conditions existing at the surface.

The conditions that are different include:

- Temperature in the test horizon is some 20°C to 30°C higher than at shallow depth;
- Pressure in the test horizon is some 9 MPa (1300 psi) higher than at the surface;
- The density of the water in the test horizon is significantly different from the density at the surface;

- The compressibility of the water in the test horizon and in the water column leading from the surface to it is different from the compressibility of water under standard conditions at the surface;

- The geochemistry of the water at the test horizon is considerably different from the geochemistry of a sample of the same water under standard surface conditions.

The vast majority of single-hole hydrogeologic tests conducted at the BWIP site have utilized uphole methods to measure hydraulic head, temperature and flow rates. The inherent assumption with uphole measurements is that they are representative of the conditions within the test interval or can be extrapolated to downhole conditions. The head and flow rate in the test interval must be known (or estimated) to calculate hydraulic parameters from test results. If frictional, compressional, thermal, and gas effects are important in deep drillholes, then head and flow data measured with uphole equipment during hydrogeologic testing may be unrepresentative of conditions within the test interval.

1.2 APPROACH

The approach of this STP is to examine, in general terms, the factors affecting the uphole measurement of head and flow rate during hydrogeologic testing in deep boreholes and to discuss the magnitude of potential errors involved in using uphole measurement techniques. Where possible within the scope of this STP, quantitative assessment using data collected at the BWIP site is made of the potential errors. However, some of the factors are poorly understood and it is necessary to assume various data and conditions in order to quantify potential errors.

1.3 SUMMARY OF DOWNHOLE MEASUREMENT METHODS USED AT BWIP

Until recently, all hydrogeologic tests conducted in boreholes on the BWIP site utilized uphole methods of measuring hydraulic head, flow rate and temperature. Hydraulic head was obtained by measuring the depth to water in the borehole by either a steel tape or electric well sounder, or by installing a shallow (e.g., 100 feet below the water surface) pressure transducer in the hole and monitoring pressure. Flow rate was measured at surface using a flow meter, weir or by measuring the time to fill a known volume. Water temperature was also measured at surface.

The hydrogeologic tests potentially affected by uphole measurements include the following (refer to RHO-BWI-MA-4).

- Constant Discharge Airlift: In this test water is withdrawn from the hole by air lift. Water level, discharge rate and temperature are measured. Recovery data following airlift are generally used for analysis.

- Constant Discharge Pumping: In this test water is withdrawn from the hole by a submersible pump (or equivalent). Water level, discharge rate and temperature are measured. Drawdown and recovery data are analyzed.

- Constant Drawdown Test: In this test a constant drawdown in the hole is maintained, generally by allowing an artesian hole to flow at ground surface. Water level (or pressure), discharge rate and temperature are measured. Discharge and recovery (shut-in) data are analyzed.

- Slug Injection/Withdrawal: In this test the static head in the hole is instantaneously increased or decreased under open hole conditions generally by displacing a slug of water.

Water levels are generally inferred from measurements using pressure transducer. Recovery data following the slug are analyzed.

- Pulse Injection/Withdrawal: In this test the static pressure in the hole is instantaneously increased or decreased (pulsed) under closed-in conditions. Water pressure is measured and recovery data following the pulse are analyzed.

- Constant Head Injection: In this test water is injected under constant-head conditions. Injection pressure and flow rate are measured and used in analysis.

Recent testing at the BWIP site has utilized downhole transducers which are capable of directly measuring pressures within the test interval. Several comparisons of uphole and downhole head data obtained during the same test are discussed in this STP.

2.0 SITE TECHNICAL POSITION

Uphole measurements of head and flow rate made during hydrogeologic testing in deep drillholes can be affected by gas, thermal, compressional and frictional effects in the well column. Thus, conditions measured at or near surface may not be representative of conditions in the interval being testing.

Evaluations of these effects presented in this STP indicate that significant errors can result when using uphole measurements to determine aquifer parameters. Potential errors are listed qualitatively in Table 2-1

Most single-hole tests conducted at the BWIP site have been monitored using uphole methods. The information presented in this STP leads to substantial questions as to the validity of data collected by uphole methods during single-hole hydrogeologic tests at BWIP. The conclusion of this study is that downhole measurements are essential to obtain reliable data upon which to base estimates of hydraulic parameters in the deep basalt units.

3.0 DISCUSSION

3.1 INTRODUCTION

The factors affecting uphole measurement of head and flow data considered significant are gas-bubble entrainment, thermal and compressional effects, and frictional head losses. Each factor is discussed below. Quantitative assessment using BWIP data is made of the potential errors involved in using uphole measurement techniques. However, the objective is not to develop techniques for modifying or "correcting" uphole measurements but to illustrate the magnitude of the errors and to stress the need to use downhole measurement techniques to avoid these possible errors.

3.2 BASIC CONCEPTS

3.2.1 Physical Properties of Water

It is important to review several of the physical properties of water that could affect the measurement of head and flow rate using uphole versus downhole equipment. In general, these properties are sensitive to temperature variations and, to a lesser extent, pressure variations. Thus, these physical properties will be different in water located at depth (e.g., 1000 m) in a borehole under in situ temperature and pressure conditions compared to water located at or near ground surface in the same borehole where different temperature and pressure conditions exist.

These physical properties and their variation with temperature are discussed below. While variations with pressure also occur, it is generally considered that the pressure dependent variations of physical properties are of a lesser magnitude than the temperature dependent variations (Bear, 1975; CRC, 1981).

Density

Fluid density (ρ) is defined as the mass of fluid per unit of volume. It varies with temperature (T) and pressure (P). Figure 3-1 shows the variation of density with temperature for water at atmospheric pressure.

Viscosity

Viscosity is a fluid property related to the extent to which the fluid resists shear when the fluid is in motion. It is defined by

$$\tau = \mu \frac{dv}{dy} \qquad (3\text{-}1)$$

where τ is the shear stress, dv/dy is the velocity gradient and μ is the dynamic viscosity (Vennard and Street, 1975). The kinematic viscosity, ν, is defined by

$$\nu = \mu/\rho \qquad (3\text{-}2)$$

Viscosity is highly dependent upon temperature as shown in Figure 3-1. It is only slightly dependent upon pressure (CRC, 1981).

Compressibility

Compressibility (β) is a measure of the change in volume (and related density) that a fluid undergoes as it is subjected to pressure changes. For isothermal conditions it is defined as

$$\beta = -\frac{1}{V}\frac{dV}{dP} = \frac{1}{\rho}\frac{d\rho}{dP} \qquad (3\text{-}3)$$

where V is the volume of a given mass of fluid, P is pressure and ρ is density (Bear, 1975). Figure 3-1 shows the variation in isothermal

compressibility at one atmosphere with temperature. Table 3-1 tabulates isothermal compressibility at one atmosphere (1.013×10^5 N/m^2) and 1000 atmospheres (1.013×10^8 N/m^2). CRC (1981) suggests that isothermal compressibility varies linearly with pressure within this pressure range.

Coefficient of Thermal Expansion

The coefficient of thermal expansion (or isobaric thermal expansion) defined at a pressure P is

$$\beta_p = -\frac{1}{\rho}\frac{d\rho}{dT} \qquad (3\text{-}4)$$

were β_p is the coefficient of thermal expansion, ρ is density and T is temperature (Bear, 1975). The variation of β_p with temperature is shown in Figure 3-1.

3.2.2 Concept of Potential

The force component acting on a fluid particle can sometimes be expressed as a negative gradient of a scalar quantity called a force potential. It is possible to define a force potential only with respect to force fields that are conservative (Hubbert, 1940) that is:

$$\oint \underline{f} \cdot \underline{ds} = 0 \qquad (3\text{-}5)$$

where $\underline{f}$ is the force and $\underline{ds}$ is the displacement in the force field, (Corey, 1977). The underline indicates a vector quantity. The integral is taken about any closed path.

If the above condition is satisfied, then a scalar force potential ϕ can be defined by

$$\Phi = \int_{\underline{s}_0}^{\underline{s}} - \underline{f} \cdot \underline{ds} \qquad (3\text{-}6)$$

where $\underline{s}$ and $\underline{s}_o$ represent the position from a datum with respect to which Φ is defined. The potential Φ is said to be conservative.

It is useful to define a potential because the negative gradient of the potential indicates the force acting at any point in the system. Forces that produce motion (driving forces) are sometimes conservative. Forces that are a consequence of motion (e.g., shear forces) result in energy dissipation and are non-conservative.

Two types of potentials are normally important in groundwater flow. These include a pressure potential, Φ_p, having dimensions of energy/volume, the negative gradient of which is the force resulting from the spatial distribution of pressure, and a gravitational potential, Φ_g, having spatial dimensions of force/mass, resulting from the gravitational acceleration upon a fluid particle.

Sometimes it is feasible to add potentials to obtain a combined potential, the negative gradient of which gives the combined force component in the direction being considered. In the case of Φ_p and Φ_g, it is not possible to combine these potentials unless density is constant or depends only on pressure (Corey, 1977).

For the special case of constant density, however, it may be convenient to combine Φ_p and Φ_g. To do so, both Φ_p and Φ_g must have the same dimensions. Two common definitions of total potential are the piezometric pressure

$$P^* = P + \rho g h \qquad (3\text{-}7)$$

where h is the elevation difference between $\underline{s}$ and $\underline{s}_o$ and P^* has dimensions of energy/volume, and the piezometric head

$$H = \frac{P}{\rho g} + h \qquad (3\text{-}8)$$

which has dimensions of energy/weight.

The distinction between pressure potential and total potential is an important one to bear in mind. Pressures measured in the borehole cannot be converted to equivalent water levels or heads unless conditions in the wellbore are known, or the density distribution is known.

3.3 DISSOLVED GAS EFFECTS

RHO has documented numerous experiences where pressures measured by uphole transducers in an open borehole were observed to rise above static pressures during the recovery period of a constant-discharge withdrawal test. RHO has explained this "overshoot" phenomenon as resulting from dissolved gas coming out of solution (due to rapid pressure decrease) and subsequently decreasing the density of water inside the riser pipe. As a result, the water level in the wellbore may be displaced by entrained gas bubbles. Entrainment of gas bubbles may significantly affect the interpretation of pressure measurements at uphole transducers. Gas overshoot response from an RHO field test is estimated in this section.

3.3.1 Maximum Gas Overshoot

The solubility of a gas in water at constant temperature is directly proportional to its partial pressure. Gas will come out of solution when its concentration in water exceeds the maximum solubility concentration for the temperature and pressure occurring at that depth. Thus, for a wellbore instantaneously filled with gas-rich water, the concentration of gas released from solution is the difference between the initial concentration and the maximum solubility concentration. A volume of water will be displaced as gas comes out of solution. The

displaced volume is related to the degassed volume, and to the pressure and temperature of the water at that depth. The general relationship between volume, pressure, temperature and mass of gas is expressed by the ideal gas law which is written mathematically as

$$PV = mRT \qquad (3\text{-}9)$$

where: P = Pressure $[ML^{-1}t^{-2}]$
V = Volume $[L^3]$
m = Mass $[M]$
R = Gas constant $[L^2T^{-1}t^{-2}]$
T = Temperature $[T]$

To calculate maximum gas overshoot, the riser pipe was divided into equal intervals of 50 meters in length and the volume of gas released from solution was estimated for each interval. The entire riser pipe was assumed to be at the temperature of the interval being tested. First, the average hydrostatic pressure at the center of each interval was calculated and the maximum solubility concentration for that pressure estimated from a solubility-pressure diagram. Knowing the initial gas concentration in the water, the amount degassed is the initial concentration minus the maximum concentration at that pressure. Using the equation of state (Eqn 3-9), the degassed volume for each interval can be estimated. Finally, summing the effects of degassing for each section, the maximum overshoot attributable to degassing can be estimated.

3.3.2 Maximum Overshoot: Field Example

Figure 3-2 shows pressure changes that were measured with a shallow transducer during the recovery period of a constant discharge pump test conducted in the Composite Umtanum Flow Top in RRL-2 (Strait and Spane, 1982). Also shown are the pressure changes measured by a downhole transducer. At 9 minutes of recovery, downhole pressure had recovered to within 3×10^{-3} MPa below the static value. However, at the same time, pressure at the shallow transducer had overshot pretest

conditions and was 1.3×10^{-1} MPa above static pressure. As recovery progressed, the pressure in the shallow transducer gradually fell to the static value.

The geometry of downhole equipment, temperature and pressure for static conditions in the Composite Umtanum Flow Top at RRL-2 are shown in Figure 3-3 (Strait and Spane, 1982). Temperature in the bottom of the water column, measured using a downhole thermal sensor was 56.6°C. Temperature at the top of the water column was estimated to be 23.4°C based upon a reasonable geothermal gradient.

The distribution of dissolved gas components in the Grande Ronde Basalt zone at borehole RRL-2 is shown in Table 3-2. Methane is the primary gas constituent comprising 97 percent by volume of the dissolved gasses sampled in the Umtanum Flow Top. For this reason, methane is assumed to be the dissolved gas in the gas overshoot response calculations. The maximum solubility concentration of methane in water as a function of pressure has been measured experimentally by Haas (1978) and is shown in Figure 3-4. Methane solubility at pressures less than 1.7×10^6 Pa are not reported and are assumed to approach zero.

The assumptions inherent in this analysis are:

- The riser pipe is instantaneously filled with methane-rich water.
- The water temperature remains constant at 56.6° C (formation temperature).
- Methane is the only gas to come out of solution.
- None of the degassed methane escapes into the atmosphere.
- Methane acts as an ideal gas.

- The water degasses instantaneously.

Maximum gas overshoot was estimated for two cases. First, the initial methane concentration was assumed to be the concentration measured and reported in Table 3-2 (.702 kg m^{-3}). Secondly, the initial methane concentration was assumed to be the maximum solubility concentration at the pressure of the test interval (1.25 kg m^{-3}). In both cases, the riser pipe was divided into 50 m intervals to perform the calculations.

For an initial methane concentration of .702 kg m^{-3}, the estimated maximum gas overshoot is 39 m above static water level. For an initial concentration of 1.25 kg m^{-3}, the estimated maximum gas overshoot is 83 m above static water level. These estimates of maximum gas overshoot indicate that dissolved gases coming out of solution may have a significant effect on observed overshoot.

Since a shallow pressure transducer (e.g., 20.7 m below static water level) was used to monitor the test response, the actual water level in the wellbore was not measured. Thus, the true density of the water/gas mixture above the shallow transducer cannot be determined. Assuming a fluid density of 1000 kg m^{-3} (i.e., no gas bubbles present) the observed pressure of 13 x 10^{-2} MPa in the shallow transducer would correspond to an overshoot of 13 m at nine minutes after airlifting stopped. The extrapolated overshoot at one minute after airlifting stopped (see Figure 3-2) would be 26 m, again assuming no gas bubbles were present. Both values are less than the calculated overshoots.

However, if gas bubbles were present in the fluid above the shallow transducer, then the effective density of the fluid was less than 1000 kg m^{-3}. For an initial methane concentration of .702 kg m^{-3}, the fluid density near the shallow transducer would be approximately 680 kg m^{-3} (calculated by the model in Section 3.3.1) which would correspond to an overshoot of 19 m at nine minutes. For an initial methane concentration of 1.25 kg m^{-3} the fluid density would be 540 kg m^{-3} and the overshoot would be 25 m according to the model.

This suggests that gas may not be released instantaneously and/or that a significant volume of degassed methane may have escaped into the atmosphere at early times in the water-level recovery. In the next section, overshoot decay due to gas bubbles escaping will be estimated.

3.3.3 Gas Overshoot Decay

Following degassing, the bubbles will travel upwards in the riser pipe, eventually escaping to the atmosphere. This will result in decay of the overshoot. In the following section, an attempt has been made to quantify the ratio of decay using data on the velocity of bubbles in water.

Peebles and Garber (1953) reported the velocity of single air bubbles in water as a function of bubble size. The results are shown on Figure 3-5. The maximum velocity of 0.33 m/s occurred for bubbles of about one millimeter radius. Larger bubbles lost their sphericity and moved upwards at a lower velocity. The tests were performed in large vessels with single bubbles. For the conditions under consideration in the wellbore, the riser pipe has a diameter of 44.5 millimeter. Maximum velocities for single bubbles of one mm diameter in the riser pipe would therefore be similar to those measured in the above noted experiment. However, in the riser pipe, it is probable that there will be multiple bubbles, and that bubbles may be initially smaller than one millimeter and subsequently expand to much greater than one millimeter, and may also coalesce. All of these factors will result in velocities by less than the maximum of .33 m/s for the one mm single bubbles. However, for calculation purposes, the maximum velocity has been used, which will tend to underestimate the decay time.

The assumptions for this estimate are:

- Methane bubbles in water act like air bubbles in water.

- The bubbles are moving uniformly and steadily at a constant velocity of 0.33 m/s throughout the well.

- Due to density differences, all the bubbles will move up the well and exit at the water surface.

- As the gas moves up the well, the bubbles will expand in response to decreasing pressure.

- Temperature effects are neglected.

- Only the gas moves.

- The water degasses instantaneously on pump shut down and no more gas is released from or dissolved into solution.

- The time necessary to remove all gas bubbles is the travel time for the lowermost bubble to reach the water surface.

The riser pipe was divided into 50 m intervals. At the chosen velocity, the gas bubbles will travel 50 m in about 150 sec. To estimate the water-level response with time, the gas bubbles in each 50 m interval were lifted 50 m every 150 sec. At the new elevation, the gas expands in response to the decreased pressure and the corresponding water-level response was estimated. Eventually, all intervals of gas bubbles exited the well. The calculated water-level response is shown in Figure 3-6.

Note that the calculated overshoot response decayed more quickly than the measured overshoot response (Figure 3-6). This difference may be due to the following:

- Temperature is not constant but decays with time;

- Velocities are not constant with depth or time;

- Gas may be redissolved due to pressure and temperature changes in the wellbore;

- Frictional, compressional, and/or other effects are not accounted for in this evaluation.

Some of these effects are addressed below.

3.4 THERMAL EFFECTS OF WATER

As mentioned in Section 3.3, RHO has attributed overshoot during the recovery period of a constant-discharge withdrawal test to dissolved gases coming out of solution as rapid pressure changes occur. Although this explanation is plausible, RHO has not considered the effects of temperature variations in the riser pipe during recovery that differ from those that existed when the static water level was measured initially.

In this discussion, overshoot response from an RHO field test is analyzed using physical models based on thermal expansion of water in the riser pipe. The purpose of these calculations is not necessarily to dispute the importance of dissolved gas in contributing to the overshoot phenomenon but to show that thermal expansion in the fluid column is significant and should be considered a contributing factor.

3.4.1 Thermal Expansion of Water Column

The differential change in water level [$d(\Delta H)$] resulting from thermal expansion of water within a differential length of the riser pipe (dz), of constant cross-sectional area, is given by

$$d(\Delta H) = \beta_p v dz \qquad (3\text{-}10)$$

where: ΔH = change in water level [L]

z = height above test interval [L]

v = change in fluid temperature [T]

β_p = coefficient of thermal expansion [T^{-1}] (defined by equation 3-4)

The total change in water level is determined by integrating equation (3-10) along the length of the water column,

$$\Delta H = \int_0^H \beta_p(z)\, v(z)\, dz \qquad (3\text{-}11)$$

where H = initial height of the water column above the test interval.

Since the riser pipe cross sectional area remains constant, the rise in water level and reduction in density cancel each other. As a result, the pressure at the base of the wellbore does not change.

3.4.2 Maximum Thermal Overshoot: Field Example

As an example, the above analysis is applied to water-level changes from the recovery period of the constant-discharge pump test conducted in the Composite Umtanum Flow Top at RRL-2 as discussed in Section 3.3.2.

For static conditions, the temperature of water in the riser pipe is assumed to be similar to the temperature of the adjacent formation, which varies approximately linearly with depth. Figure 3-7 shows expected temperature distributions in the water column for static conditions and at the beginning of the recovery period. The temperature change (from static conditions) at some height (z) above the test section in the riser pipe is given by

$$v_o(z) = T_a - T_f(z) \qquad (3\text{-}12)$$

where: v_o = initial temperature change during recovery [T]

T_a = aquifer temperature [T]

T_f = formation temperature at static conditions [T]

Therefore:

$$v_o(z) = M_1 z \qquad (3\text{-}13)$$

where $M_1 = 3.17 \times 10^{-2}$ °K m^{-1} for this test (see Figure 3-7) and z = height above the test section. M_1 is the thermal gradient in the wellbore under static (pre-test) conditions.

Figure 3-8 shows the relationship between the coefficient of thermal expansion, and temperature. For practical purposes, the relationship can be assumed linear. Because temperature is a linear function of height above the test section, the coefficient of thermal expansion can also be assumed to be linearly related to height. The coefficient of thermal expansion is assumed to be relatively unaffected by the pressure conditions encountered in this field example. Therefore,

$$\beta_p(z) = M_2 z + B_2 \qquad (3\text{-}14)$$

where $M_2 = -2.6 \times 10^{-7}$ m^{-1} °K^{-1} and $B_2 = 5.09 \times 10^{-4}$ °K^{-1} for this test (see Figure 3-8).

If hydraulic recovery is very rapid, equation (3-10) can be used to calculate the initial (maximum) overshoot. Substitution of equations (3-13) and (3-14) into equation (3-11) results in

$$\Delta H_{max} = \int_0^H \{M_1 M_2 z^2 + M_1 B_2 z\}\, dz \qquad (3\text{-}15)$$

After integration, the final equation is

$$\Delta H_{max} = \frac{M_1 M_2 H^3}{3} + \frac{M_1 B_2 H^2}{2} \qquad (3\text{-}16)$$

Using the values noted above for this test, the maximum calculated overshoot (ΔH_{max}) is 5.5 meters. This value corresponds to roughly half the observed overshoot calculated from the uphole pressure transducer and an assumed water density of 1000 kg m^{-3}. It indicates that thermal expansion of water can play a significant role in causing the overshoot phenomenon.

3.4.3 Thermal Analysis of Overshoot Decay

Since both groundwater flow in a porous medium and conductive heat flow are described by Laplace's Equation, solutions can be used interchangeably, with suitable definition of parameters. Analysis of overshoot decay has been performed using a thermal equivalent of the Theis semilog well recovery method. As shown in Figure 3-9, this model is composed of an aquifer from which groundwater is withdrawn and a thermal medium (i.e., formations surrounding the borehole) which conducts heat away from the borehole. During the pumping period, high-temperature groundwater flows up the well and is assumed to cause an instantaneous temperature change inside the borehole.

When groundwater withdrawal from the aquifer terminates, it is assumed that heat flux into the thermal medium instantaneously drops to zero. As a result, the temperature of the medium (and water in the well) decays to the pretest temperature (T_f). Thus, the residual temperature change inside the borehole decays from an initial value of $v_o(z)$ (at the end of the pumping) and approaches zero at late recovery times. If a small section of the borehole is approximated as a vertical line sink, the temperature decay is given by the thermal equivalent of the Theis semilog equation for well recovery,

$$v(z) = \frac{2.303\ F(z)}{4\pi K} \log (t/t') \qquad (3\text{-}17)$$

where: $v(z)$ = residual temperature change inside the borehole during recovery at height z above the test section [T]

$F(z)$ = heat flux [$ML^{-3}t^{-3}$]

K = thermal conductivity of medium [$ML^{-3}t^{-3}T^{-1}$]

t = time since beginning of heat injection [t]

t' = time since beginning of recovery [t]

The assumption that the heat flux instantaneously drops to zero at the beginning of recovery is not strictly valid because water in the borehole has heat storage capacity. However, the effects of wellbore heat storage diminish with time during the recovery period.

If hydraulic recovery in the aquifer is very rapid compared to the thermal decay, an expression for decay of the overshoot is given by substituting equation (3-17) into equation (3-11) to get

$$\Delta H = \frac{2.303}{4\pi K} \log(t/t') \int_0^H \beta_p(z)\, F(z)\, dz \qquad (3\text{-}18)$$

As an approximation, it can be shown that, for steady state conditions

$$F(z) = \frac{2\pi K v_o(z)}{C} \qquad (3\text{-}19)$$

where C is a shape factor defined by $C = \ln r_o/r_w$

and r_o = radius of influence [L]

r_w = radius of well [L]

The assumption of a constant flux rate is not strictly valid, since theory dictates that F will gradually decrease during the heat-injection period. However, in this case the thermal recovery response is relatively insensitive to minor variations in the flux rate. To

calculate a shape factor (C), a radius of influence (r_o) must be assumed. Since r_o is contained in a logarithmic term, the calculated shape factor is relatively insensitive to large variations in the assumed radius of influence. For practical purposes, r_o is assumed to be 50 times the well radius, giving a shape factor equal to 3.9.

Substituting equation (3-19) in (3-18)

$$\Delta H = \frac{2.303}{2C} \log (t/t') \int_0^H \beta_p(z)\, v_o(z)\, dz \qquad (3\text{-}20)$$

However, the term in the integral is equal to the maximum overshoot ($^{\Delta H}max$) when $v_2 v_o$. Thus

$$\Delta H = \frac{2.303\ \Delta H_{max}}{2C} \log(t/t') \qquad (3\text{-}21)$$

This equation indicates that a semilog plot of ΔH vs. log (t/t') should be a straight line passing through the point ($\Delta H = 0$, $t/t' = 1$). The slope of the semilog straight line is given by

$$\Delta H^* = \frac{2.303\ \Delta H_{max}}{2C} \qquad (3\text{-}22)$$

where ΔH^* = change in water level per log cycle of the (t/t') time parameter [L]

Since K does not exist in equation 3-21, thermal conductivity cannot be calculated from overshoot recovery data. However, a predicted value of ΔH^* can be calculated.

3.4.4 Thermal Overshoot Decay: Field Example

As an example equation (3-21)has been applied to conditions encountered in the Composite Umtanum Flow Top in RRL-2. Substitution of ΔH_{max} = 7.2 meters and C = 3.9 into equation (3-22) gives a predicted ΔH^* value of 1.6 meters.

In Figure 3-10, water-level overshoot data for the Composite Umtanum Flow Top are plotted on the semilog format. Uphole transducer pressures have been converted to heads using an assumed constant density of 1000 kg m^{-3} to permit comparison with the calculated values. Since early recovery data were probably affected by wellbore conditions, the semilog straight line was fit to later time data (e.g., small t/t' values). Use of this procedure gives a ΔH^* value of 2.2 meters which is close to the value predicted by the thermal model (1.6 meters).

In this example, the observed overshoot recovery response was similar to the predicted response based on a physical model of thermal conditions in the borehole. The results suggest that thermal expansion of water in the riser pipe may be a significant factor in controlling overshoot decay. The effects of degassing and thermal decay may be occurring at the same time in recovery tests.

3.5 COMPRESSIBILITY EFFECTS

Strait and Spane (1982) analyzed pressure oscillations during slug injection/withdrawal tests at the composite Umtanum Flow Top in RRL-2 using the Van der Kamp method. This method of analysis attributes system compressibility only to the formation. The following analysis examines the effects of wellbore compressibility.

3.5.1 Gas Compressibility Effect

Sources of wellbore compressibility may include packers, riser pipe, water, and gas bubbles in the well column, causing the column to act as a non-rigid body. Effects due to compressibility of packers and the riser pipe are unknown. In this section, the compressibility of water containing gas bubbles is estimated.

The assumptions necessary for the following estimates are:

- Solubility of the gas is neglected. In other words, the gas neither dissolves nor comes out of solution during the slug test.
- Gas is distributed uniformly (by volume) throughout the well.
- Volume changes are due only to changes in pressure.
- The compressibility of the gas/water mixture is the percent of gas in the mixture times the compressibility of gas.
- Water is incompressible compared to the compressibility of gas.
- Conditions are isothermal with the static temperature distribution shown in Figure 3-7.
- Methane behaves as an ideal gas.

For an ideal gas under isothermal conditions, the coefficient of compressibility, β, is the reciprocal of the gas pressure (Bear, 1975), such that

$$\beta = \frac{1}{P} \qquad (3\text{-}23)$$

Where P is measure in Pa. The coefficient of compressibility for methane and for methane/water mixtures was estimated for each interval in the riser pipe. These results are shown on Figure 3-11. The compressibility of pure water is also shown for comparison.

Note that the compressibility of a methane/water mixture with even one percent methane bubbles shows a marked increase in compressibility over pure water alone. Thus, analytical solutions for slug test response which ignore wellbore compressibility could be significantly in error. The compressibility of packers and the riser pipe will contribute to this error.

3.6 FRICTIONAL EFFECTS

Frictional effects may cause uphole head measurements to be unrepresentative of conditions in the test section. Frictional losses will occur in the riser pipe and through any downhole valving or packers. In this section, frictional losses are estimated to evaluate whether frictional losses, it demonstrates that frictional losses can be significant and should be considered when interpreting uphole measurements of head.

RHO used a variety of equipment and packer arrangements in hydrologic testing at RRL-2. Therefore, based on information from Strait (1984, personal communication) an arrangement of equipment was selected as representative of the possible sources of frictional losses in testing equipment. A schematic of this equipment and the relevant dimensions are shown in Figure 3-12. The four sources of frictional losses considered were:

1. The annular space between the recorder probe and the carrier sleeve;

2. The upper sub on the recorder carrier;

3. The shut-in tool;

4. The riser pipe.

Each of these sources are analyzed by methods described in Appendix A. In each case, frictional losses were estimated as a function of flow rate.

The total frictional head loss in the wellbore is the sum of the losses from each source considered. Any additional equipment in the borehole would increase frictional losses further. Figure 3-13 shows total estimated frictional head loss as a function of flow rate. Also shown is the head loss due to friction in the riser pipe alone. Note that frictional head losses in the riser pipe, which are the most easily estimated, account for greater than 50 percent of the total estimated losses. For a flow rate of about 6×10^{-4} m^3s^{-1}, approximately the flow rate used in RHO pump tests in the Composite Umtanum Flow Top at RRL-2 (Strait and Spane, 1982), total frictional losses are about 7 m. This minimum estimated frictional head loss is significant. Although frictional losses can be estimated it is normal practice to calibrate equipment for frictional losses so that losses can be considered in the analysis fo test data. To our knowledge this has not been done at the BWIP site.

TEMPERATURE VARIANT PROPERTIES OF WATER (AT ATMOSPHERIC PRESSURE)

Figure 3-1

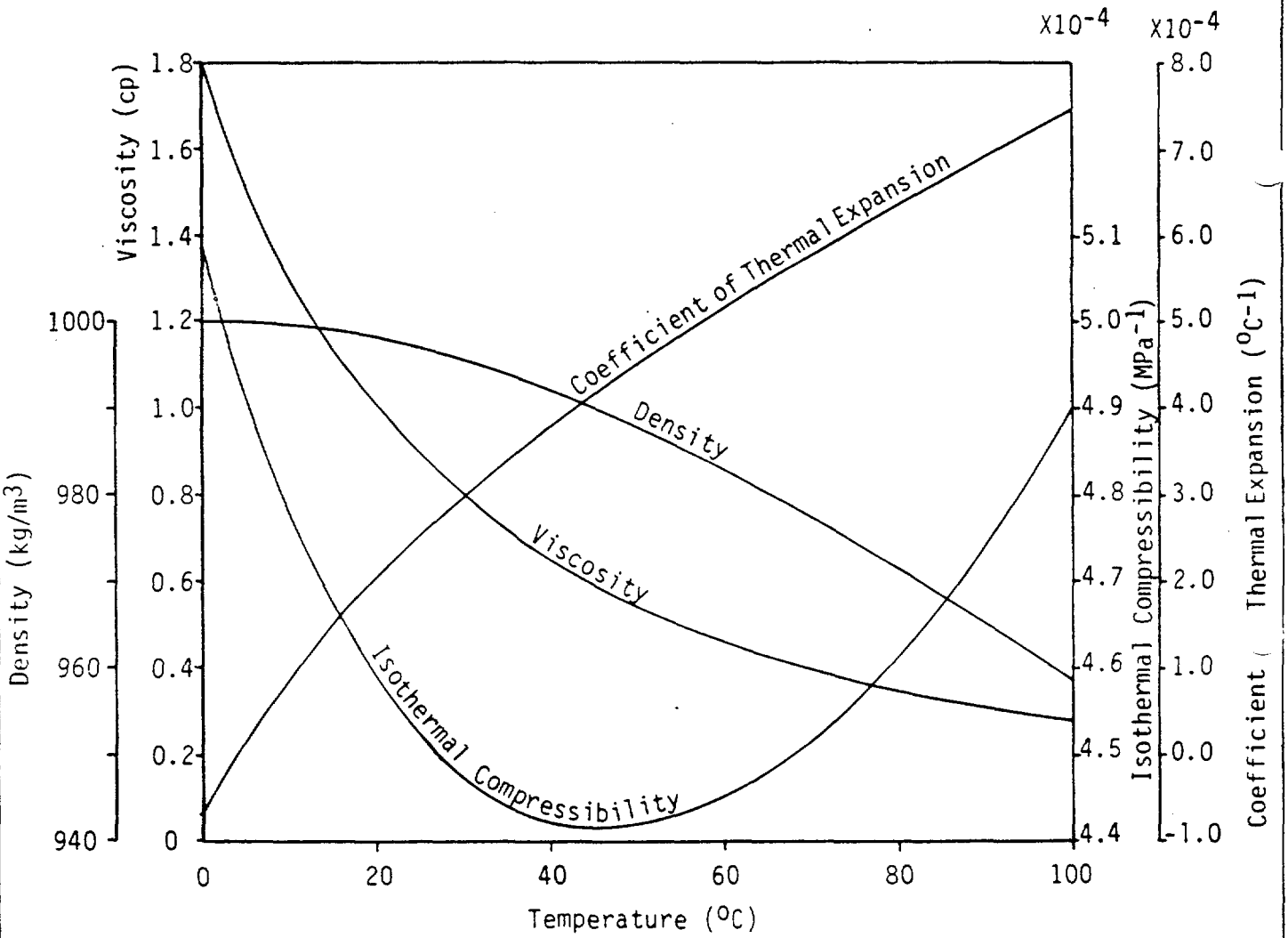

Source: CRC, 1981

Rev. ____ Dwg. No. 023-1033 ____ Date 8-16-84 Eng. P.F.

Rev.
Dwg. No. 823-1033 Date 8-20-84 Eng. P.F.

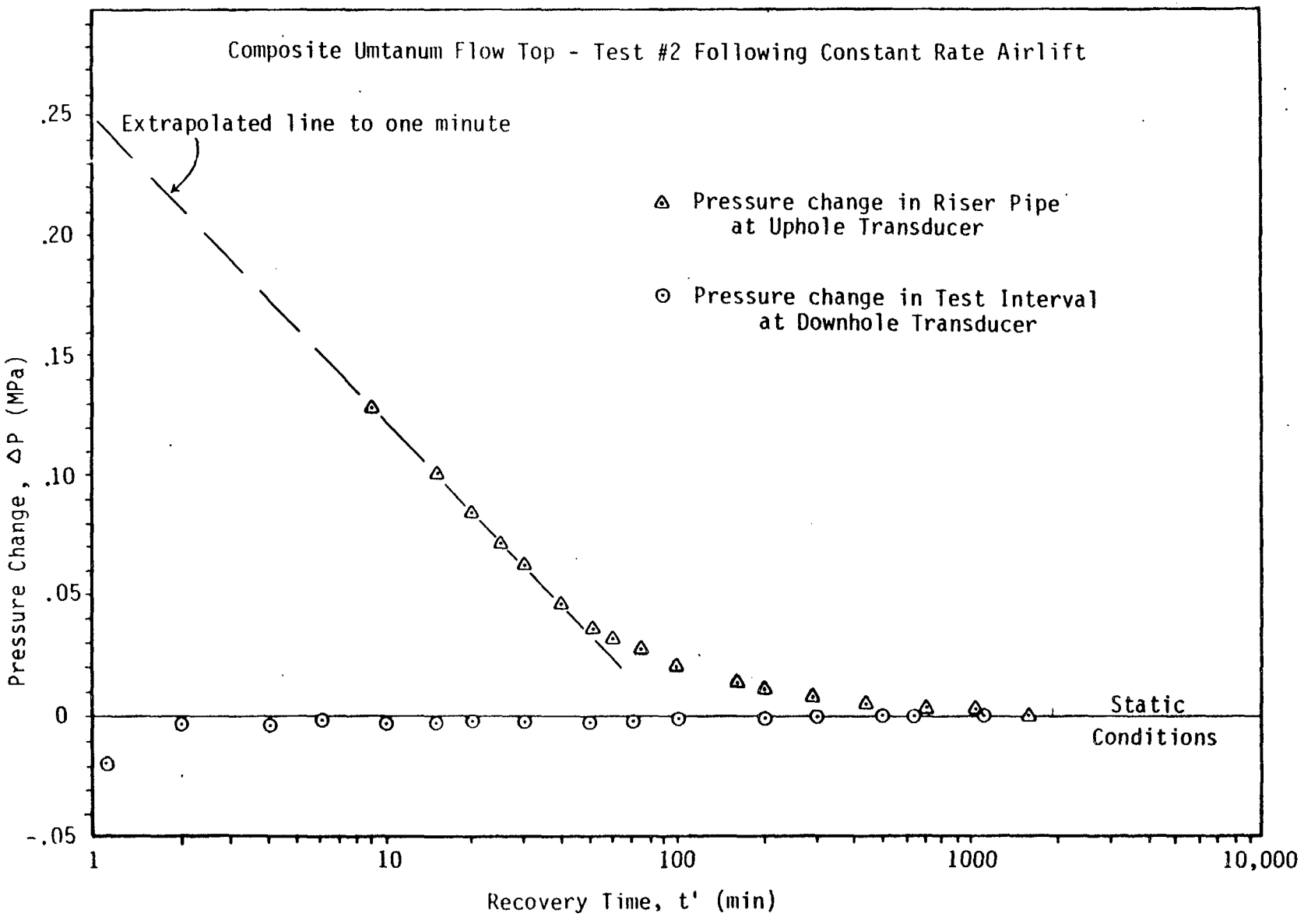

RECOVERY RESPONSE FOR COMPOSITE UMTANUM FLOW TOP IN RRL-2

Figure 3-2

Golder Associates

STATIC CONDITIONS FOR COMPOSITE UMTANUM FLOW TOP IN RRL - 2

Figure 3-3

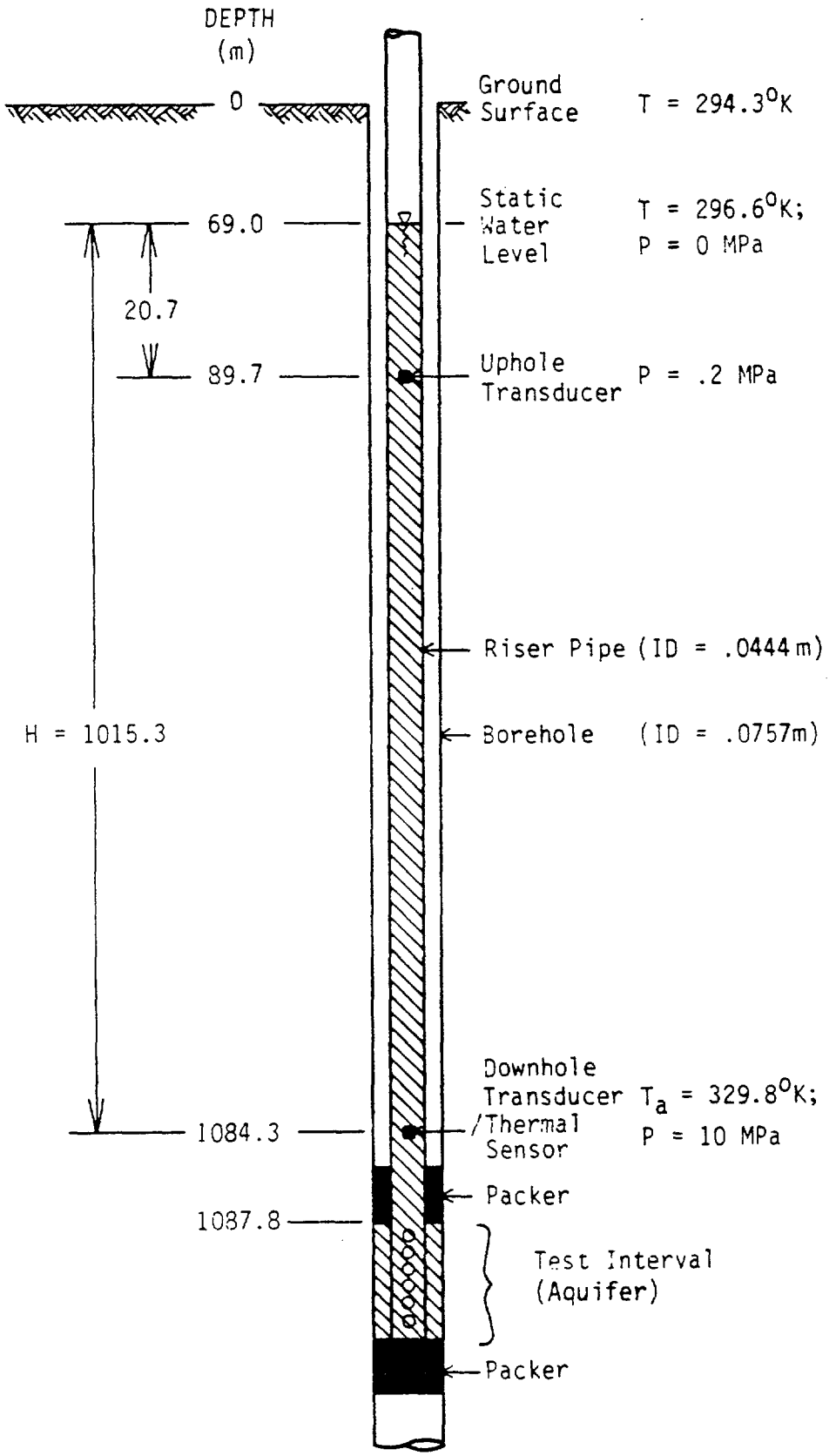

Not to scale

Rev. ____ Dwg. No. 823-1032 Date 8-15-84 Eng. P.F.

EXPERIMENTAL RESULTS OF MAXIMUM METHANE SOLUBILITY IN WATER AS A FUNCTION OF PRESSURE

Figure 3-4

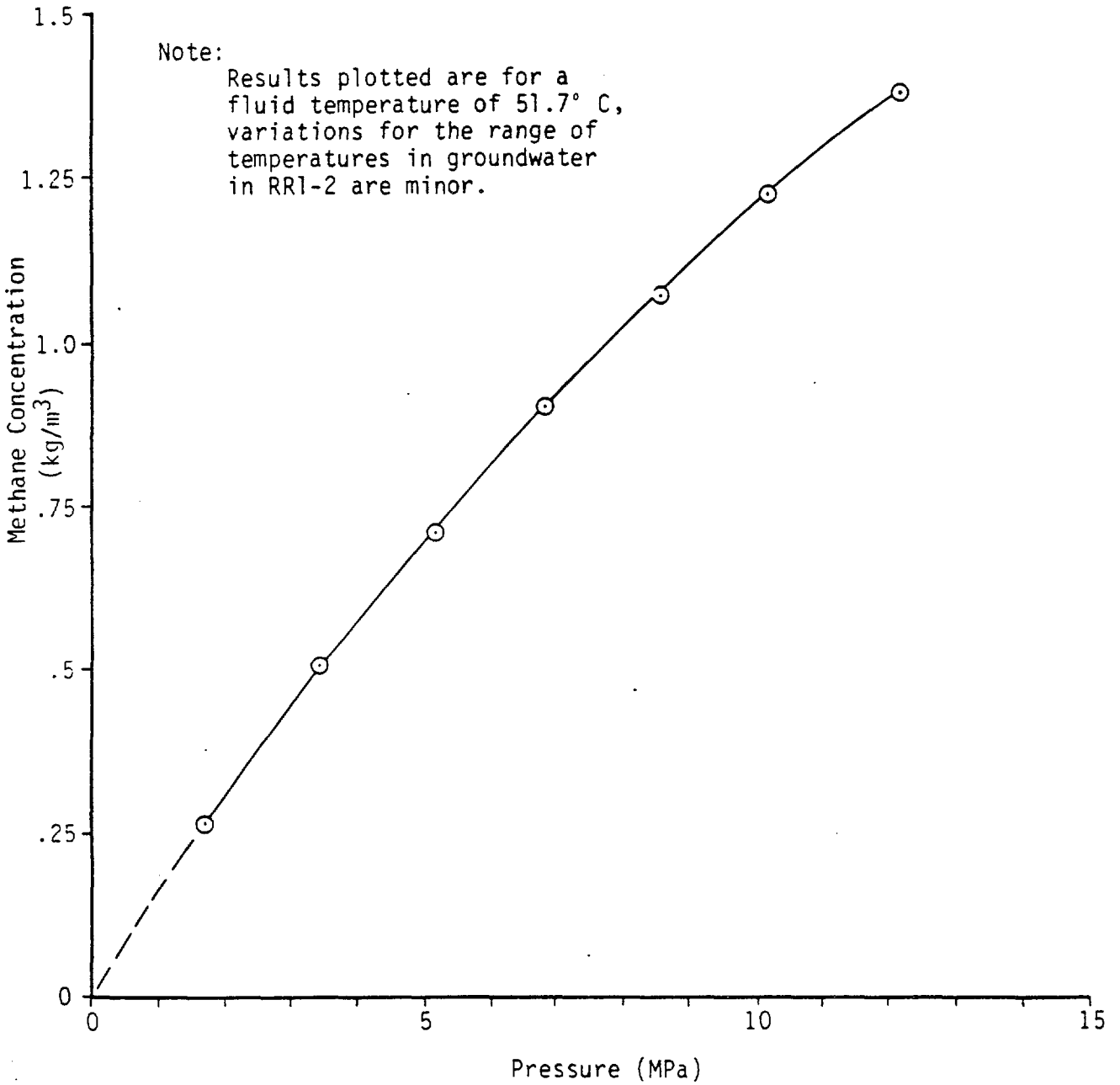

From Haas, 1978

Rev. Dwg. No. 823-1033 Date 8-15-94 Eng. PF

Rev.
Dwg. No. 823-1033 Date 8-15-84 Eng. P.F.

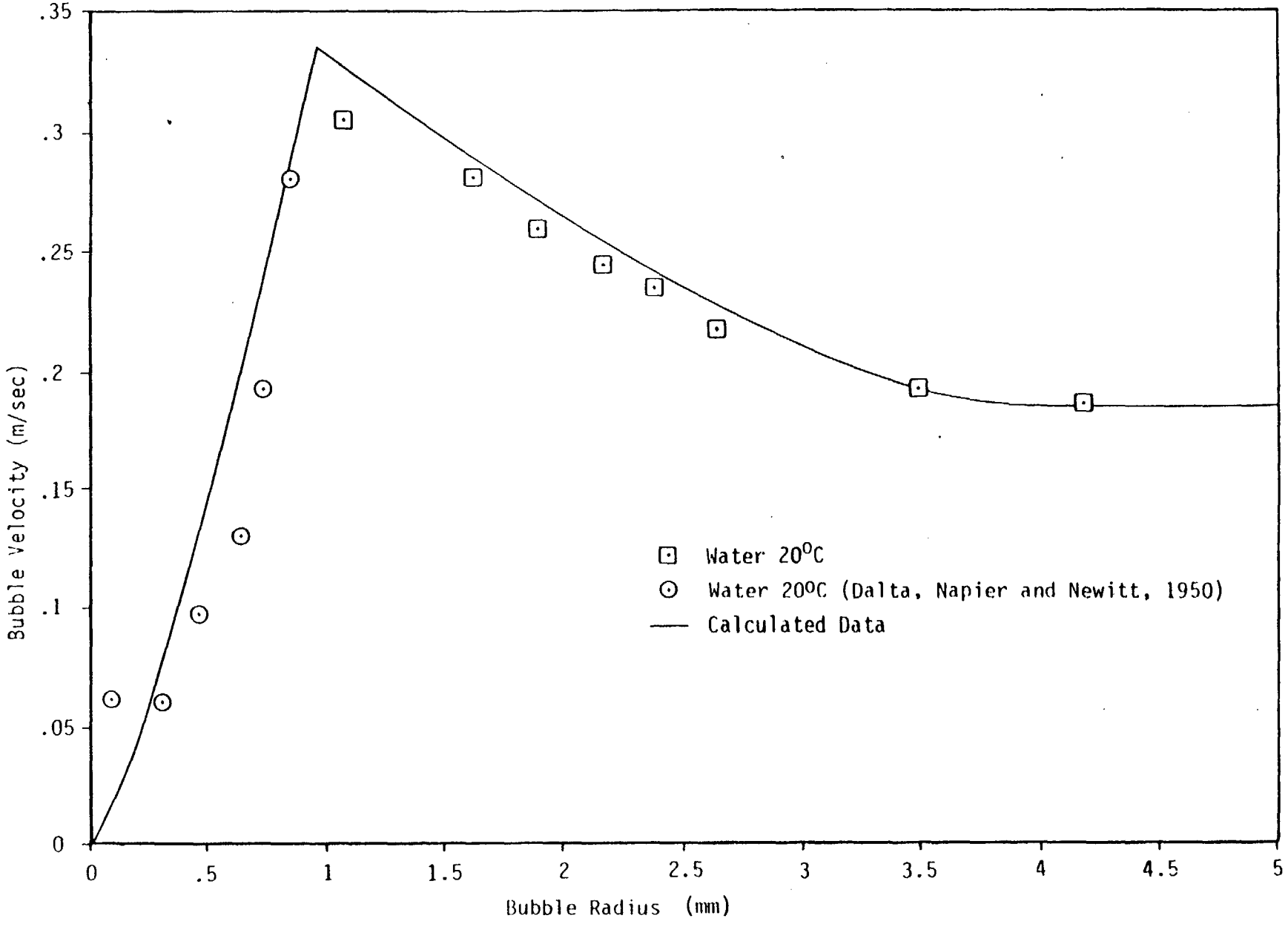

TYPICAL RESULTS OF GAS-BUBBLE VELOCITY AS A FUNCTION OF BUBBLE RADIUS

Figure 3-5

After Peebles and Garber, 1953

Golder Associates

OVERSHOOT DECAY DUE TO GAS BUBBLES EXITING WELL Figure 3-6

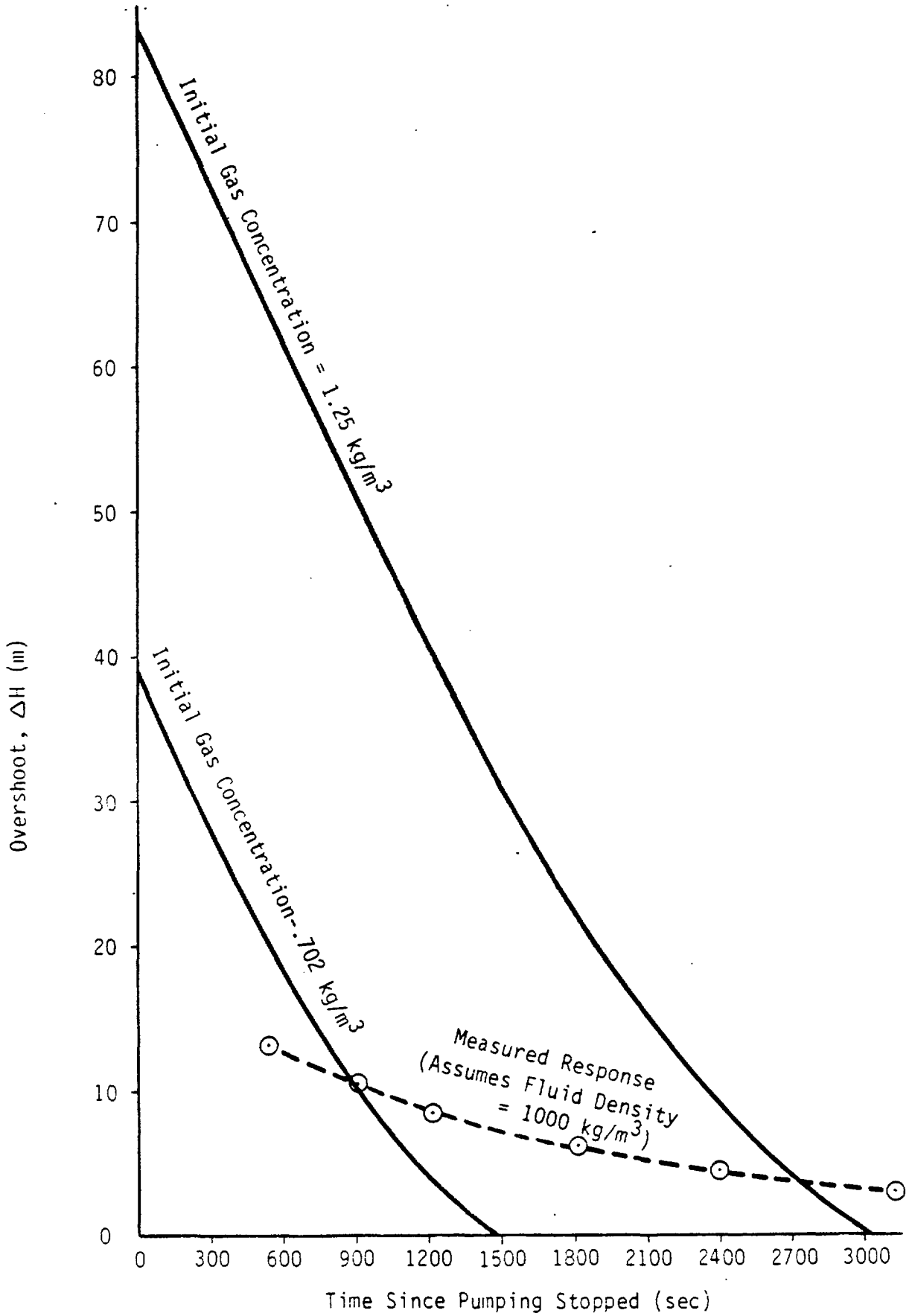

Golder Associates

Rev. ____ Dwg. No. 823-1033 ____ Date 8-14-84 Eng. P.F.

THERMAL DISTRIBUTION IN WATER COLUMN

Figure 3-7

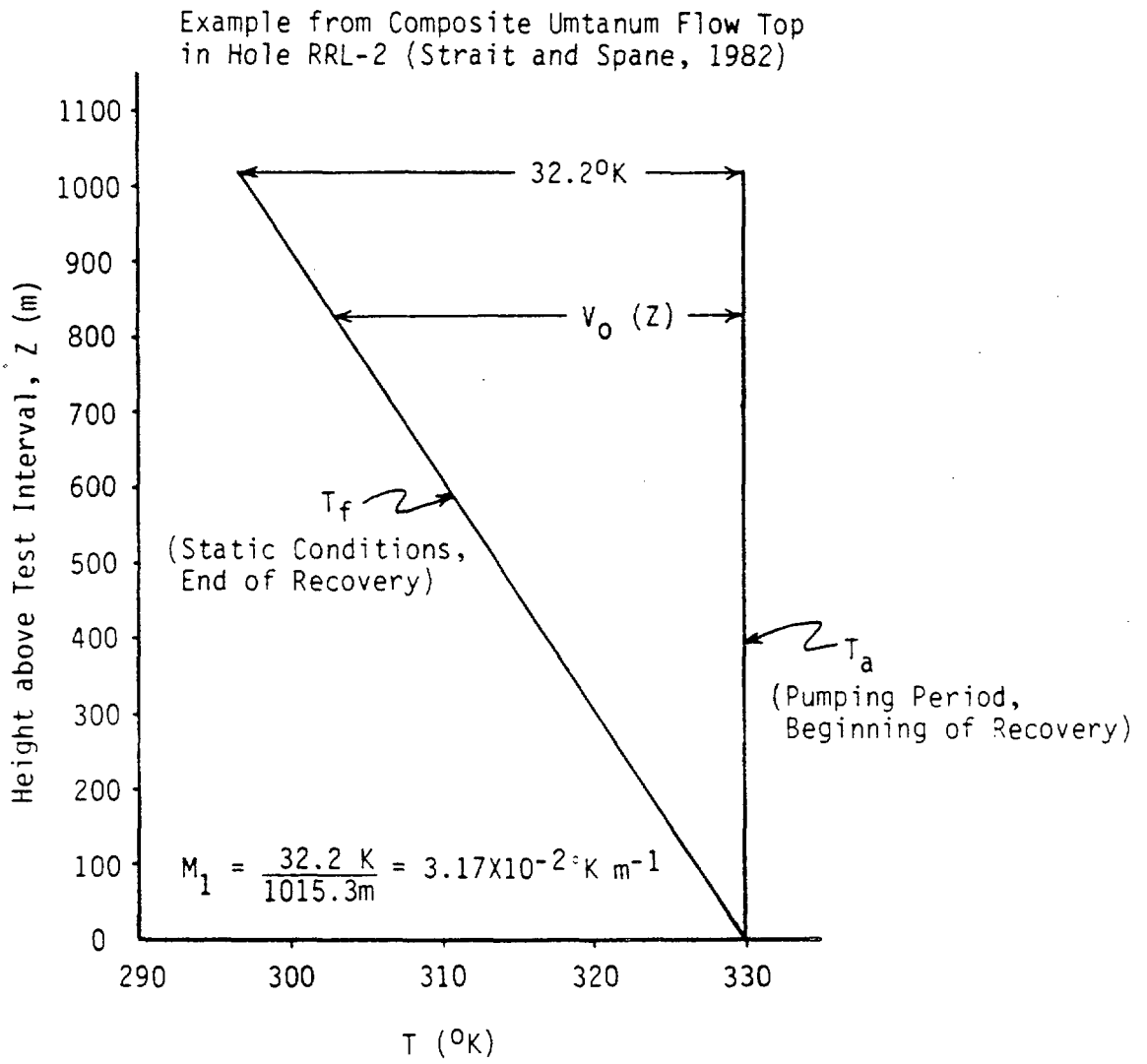

Rev. ____ Dwg. No. 823-1033 Date 8-16-84 Eng. P.F.

COEFFICIENT OF THERMAL EXPANSION (βp) VS. TEMPERATURE (T) AND HEIGHT ABOVE TEST SECTION (Z)

Figure 3-8

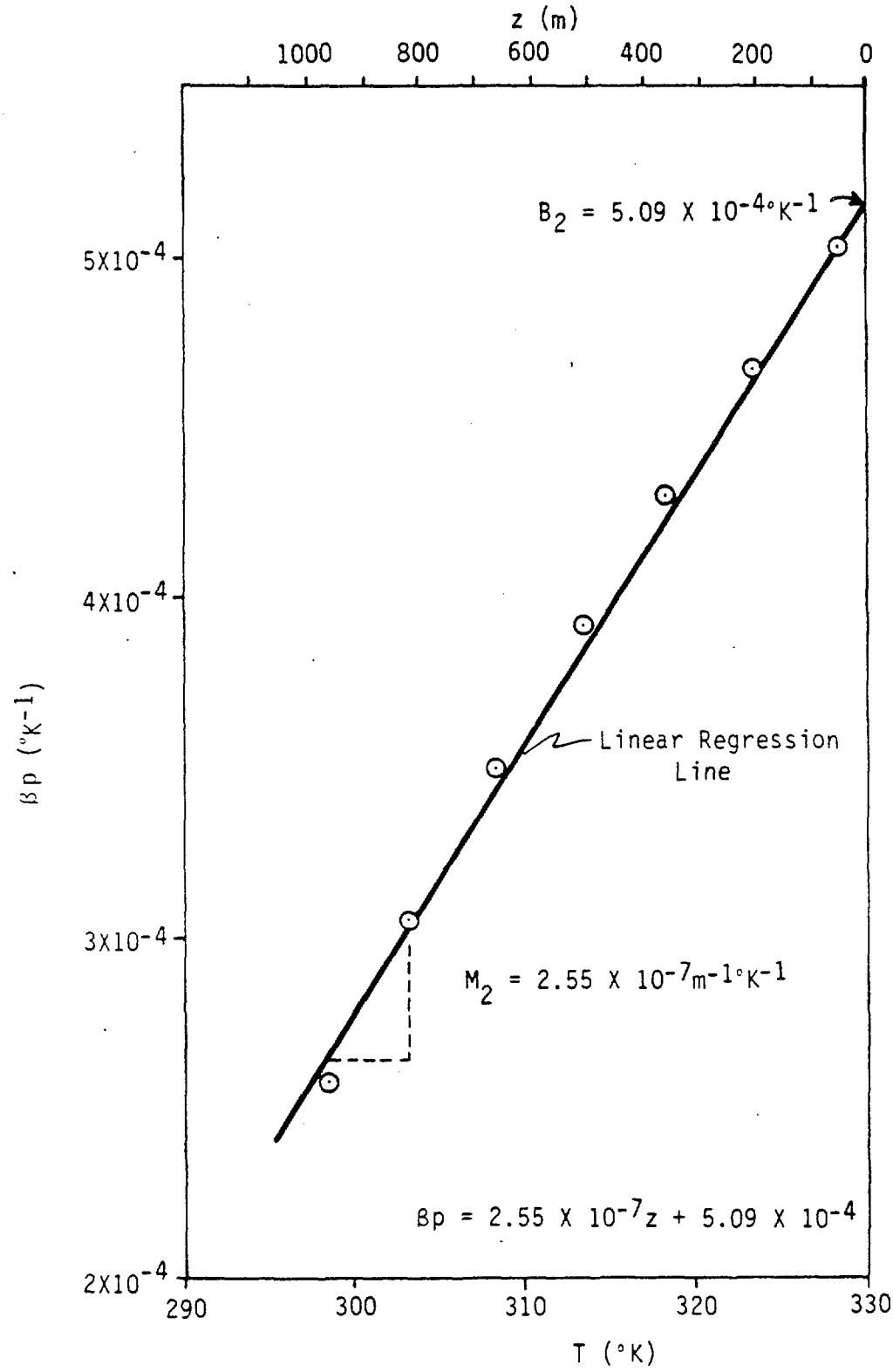

Source: CRC, 1981

Rev. — Dwg. No. 823-7033 Date 8/27/84 Eng. EF

PHYSICAL MODEL FOR THERMAL ANALYSIS

Figure 3-9

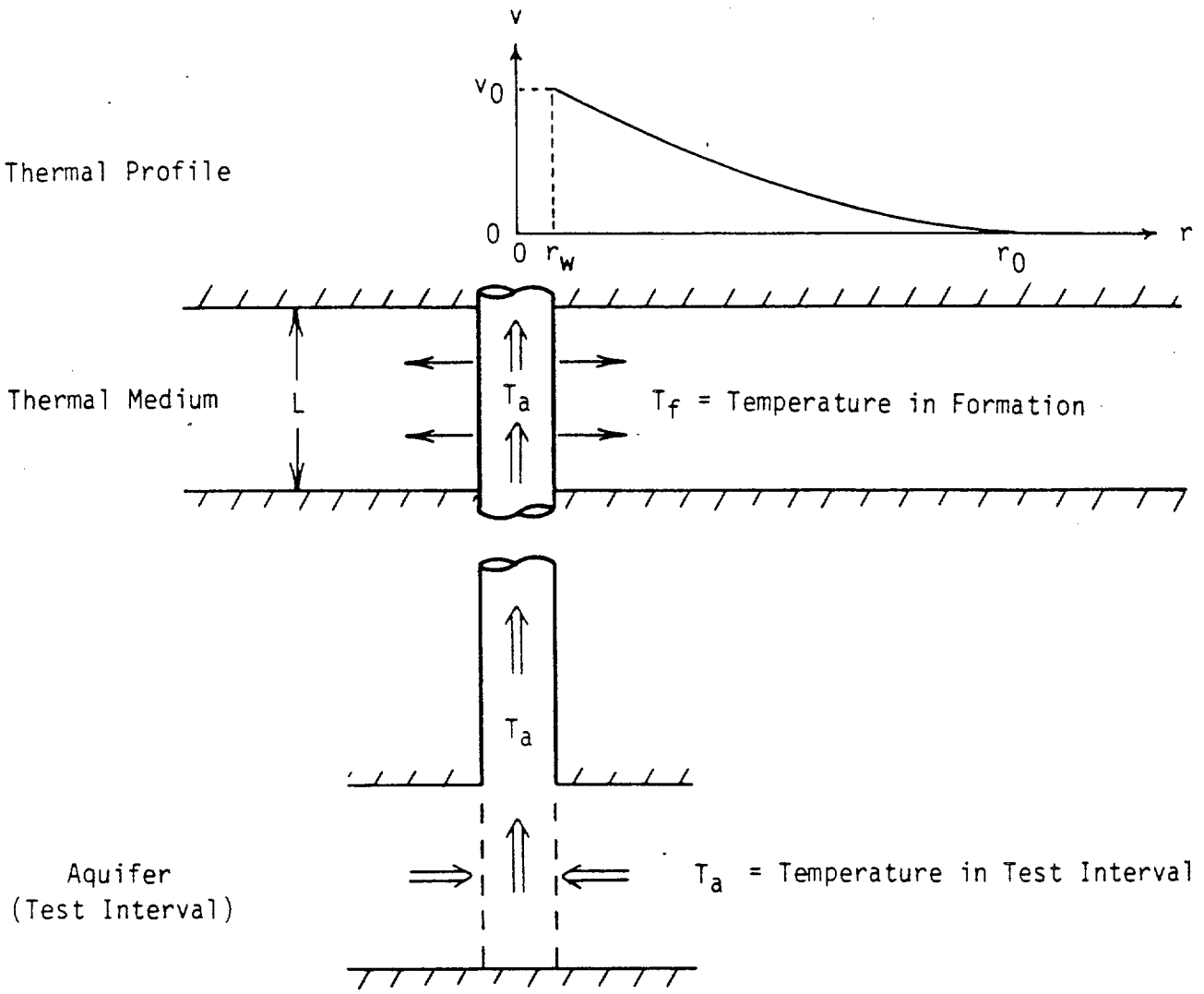

Rev. ____ Dwg. No. 823-1033 Date 12-16-84 Eng. P.F.

Rev.
Dwg. No. 823-1033 Date 8-20-84 Eng. P.F.

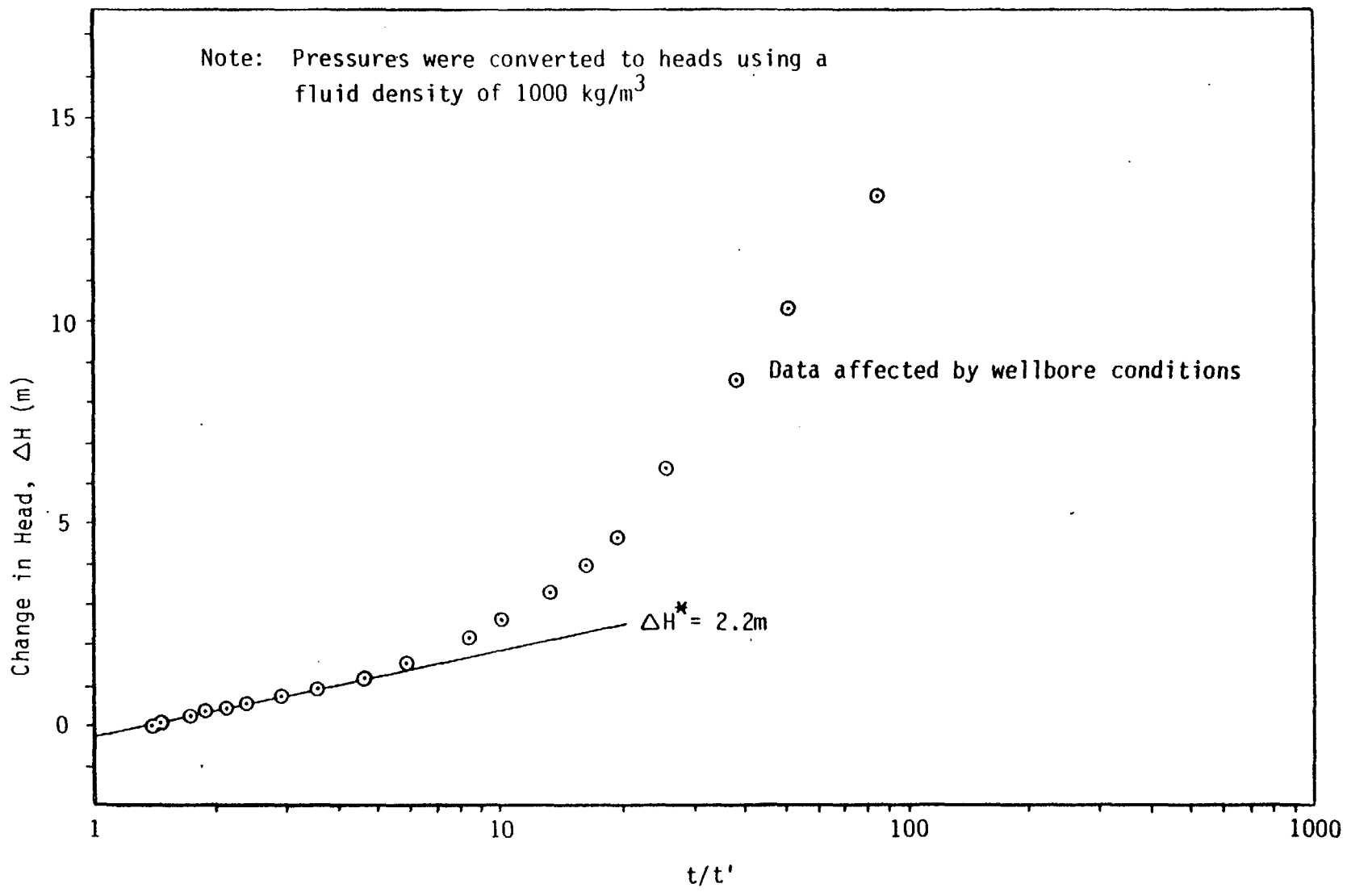

SEMILOG RECOVERY PLOT FOR UMTANUM FLOW TOP IN RRL-2

Figure 3-10

Golder Associates

CALCULATED COMPRESSIBILITY AS A FUNCTION OF PERCENT GAS VS. DEPTH

Figure 3-11

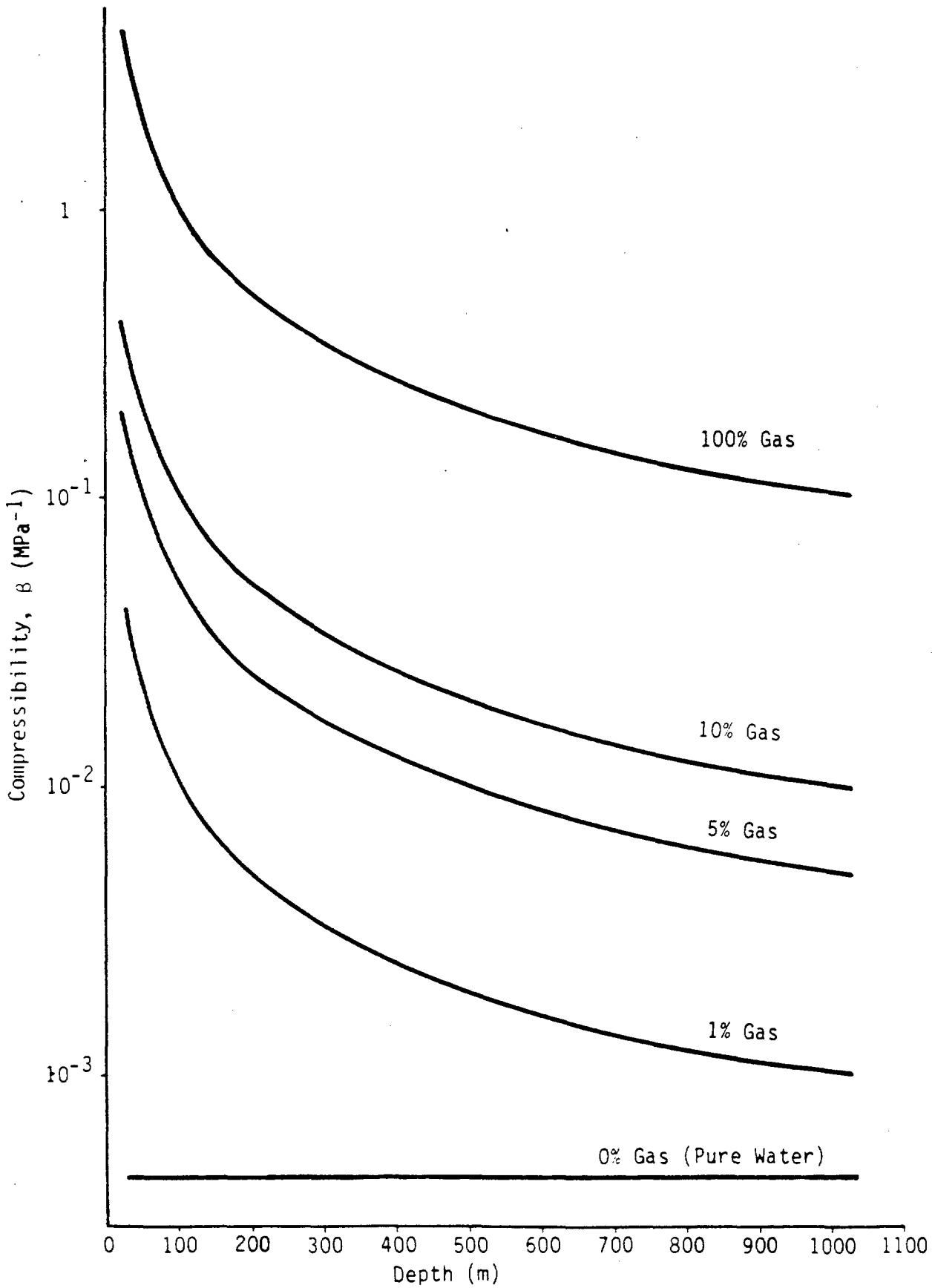

Golder Associates

Rev. —
Dwg. No. 823-1033 Date 8-16-84 Eng. P.F.

SCHEMATIC OF POSSIBLE SOURCES OF FRICTIONAL HEAD LOSSES

Figure 3-12

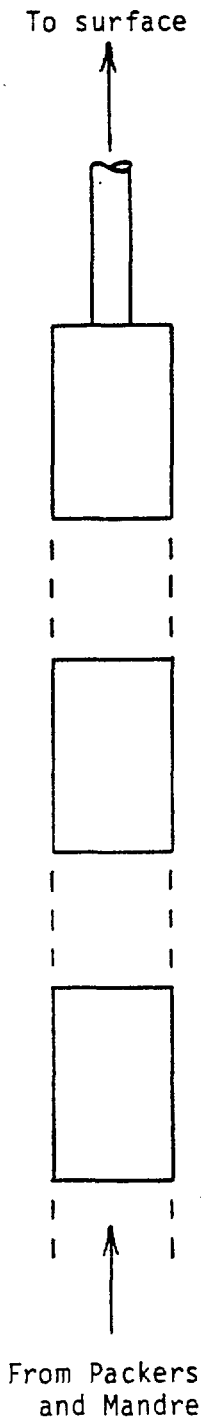

Riser pipe
Diameter $D_RP = 4.45 \times 10^{-2}$m
Length $L = 1015$ m

Six Slits in Shut-In Tool
Height $h = 4.45 \times 10^{-2}$m
Width $w = 6.35 \times 10^{-3}$m
Length $L_{SI} = 1.02 \times 10^{-3}$m

Three vertical cylindrical holes in Upper Sub
Diameter $D = 9.53 \times 10^{-3}$m
Length $L_{US} = 1.02 \times 10\text{-}1$m

Annular space between probe carrier and carrier sleeve
Outer Radius of Carrier $r_1 = 2.62 \times 10^{-2}$m
Inner Radius of Sleeve $r_2 = 2.86 \times 10^{-2}$m
Length $L_{AS} = 1.2$ m

Rev. Dwg. No. 823-1032 Date 9-20-84 Eng. P.F.

ESTIMATED FRICTION HEAD LOSS VERSUS FLOW RATE Figure 3-13

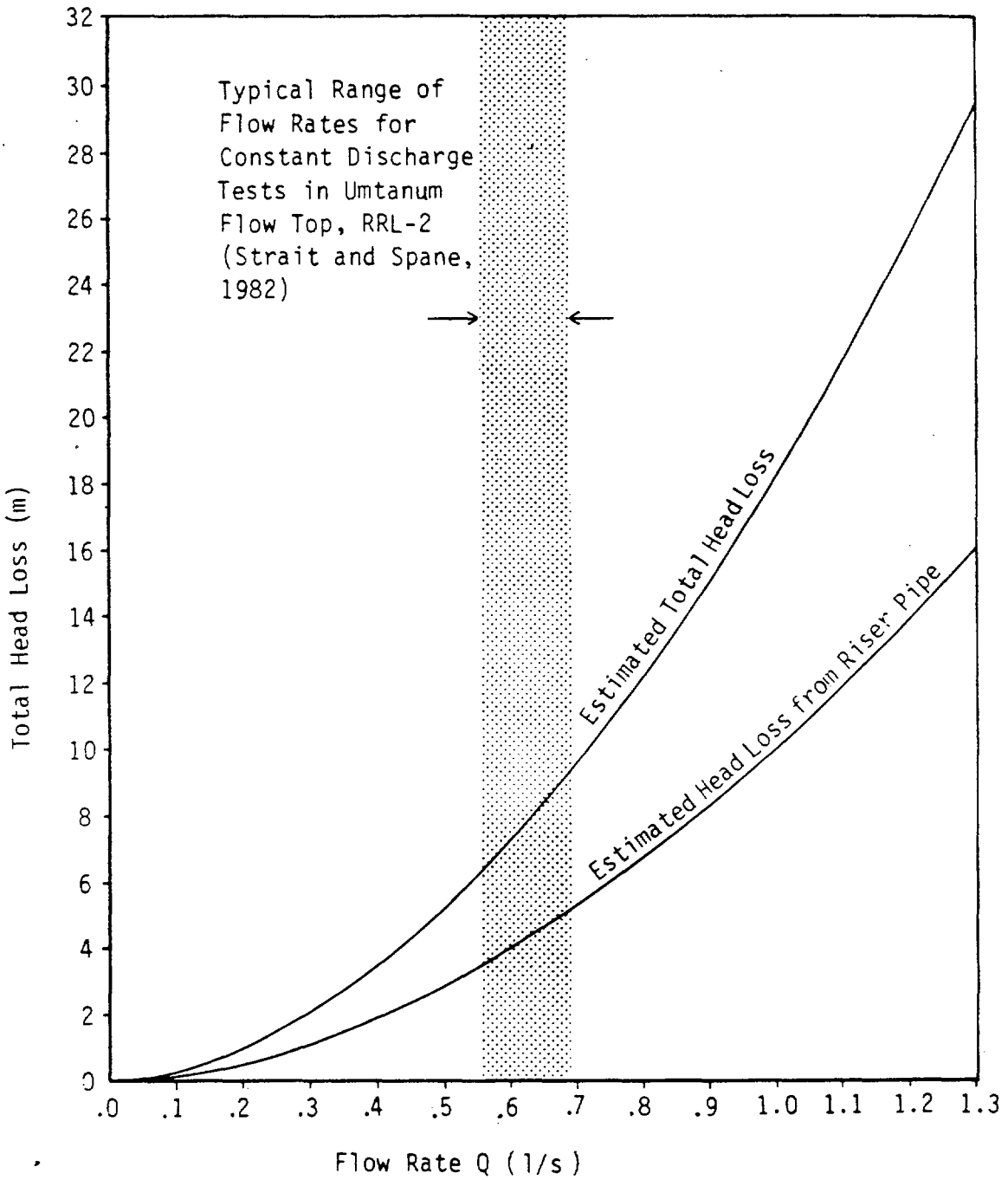

Rev. Dwg. No. 823-1023 Date 8-15-84 Eng. P.F.

Table 2-1

POTENTIAL WELLBORE EFFECTS IN DEEP HOLES

Effects	Constant Discharge Airlift	Constant Discharge Pumping	Constant Drawdown	Slug Injection/ Withdrawal	Pulse Injection/ Withdrawal	Constant Head Injection
1. Thermal						
Warm water is being withdrawn from the hole, thermal decay of the warm water column will cause density changes. Or cold water is injected at surface also causing density changes at depth.	Uphole heads not representative, Overshoot on recovery	Uphole heads not representative, Overshoot on recovery	Uphole heads not representative, Overshoot on recovery			Uphole heads not representative, density changes occurring at depth
2. Gas						
Water with dissolved gas is being withdrawn from depth, degassing will occur as pressure decreases, entrainment of gas bubbles will cause density changes.	Same as above	Same as above	Same as above			
3. Compressibility						
Sources of wellbore compressibility include packers, riser pipe, water, effects of dissolved gases and gas bubbles in the well column, well column cannot be treated as a rigid body.				Uphole heads and flow rates not representative	Uphole heads and flow rates not representative	
4. Friction						
Friction loss will occur in riser pipe and through any downhole valving or packers.	Uphole heads not representative	Uphole heads not representative	Uphole heads not representative	Uphole heads not representative		Uphole heads not representative

Table 3-1

Isothermal Compressibility of Water (MPa^{-1})

Temp °C	At 1 Atmosphere (1.013×10^{-1} MPa)	At 1000 Atmospheres (1.013×10^{3} MPa)
25	4.57×10^{-5}	3.48×10^{-5}
35	4.48×10^{-5}	3.42×10^{-5}
45	4.41×10^{-5}	3.40×10^{-5}
55	4.44×10^{-5}	3.40×10^{-5}
65	4.48×10^{-5}	3.42×10^{-5}
75	4.55×10^{-5}	3.47×10^{-5}
85	4.65×10^{-5}	3.53×10^{-5}

Source: CRC, 1981

APPENDIX A

Estimation of Frictional Losses in Downhole Equipment

A.1 Frictional Head Loss in the Annular Space

During pumping, groundwater flows from the formation through the mandrill and into the downhole equpment. Frictional losses in the mandrel are not known. Water then flows through an annular space between the probe carrier and the sleeve of the carrier. From there the water flows into the upper sub. In this section, frictional losses into, through, and out of the annular space in the probe carrier are estimated.

For turbulent flow in non-circular conduits (Roberson and Crowe, 1980),

$$h_f = \frac{f\ L_{AS}\ V^2}{4\ A_T/P\ 2g} \qquad (A\text{-}1)$$

where:

h_f = frictional head loss [L]

f = friction factor

$= 0.316\ Re^{-.25}$

L_{AS} = length of annular space [L]

A_T = total cross-sectional area [L^2]

P = wetted perimeter [L]

g = gravitational acceleration [Lt^{-2}]

V = velocity [Lt^{-1}]

$= Q/A_T$

Q = flow rate [L^3t^{-1}]

Re = Reynolds number

$= \frac{4\ V\ A_T}{P\nu}$

ν = kinematic viscosity [L^2t^{-1}]

Entrance and exit head losses are given by (Roberson and Crowe, 1980)

$$h_f = \frac{KV^2}{2g} \qquad \text{(A-2)}$$

where: K = loss coefficient
= 1.0 for outlet
= 0.5 for sharp-edged inlet

For this case, $A_T = \pi (r_2^2 - r_1^2)$ and $P = 2\pi (r_1 + r_2)$ where r_1 = outer radius of probe [L] and r_2 = inner radius of carrier sleeve [L]. Therefore, the frictional head loss for flow through an annular space as a function of flow rate is given by

$$h_f = \frac{f L_{AS} Q^2}{4\pi^2 g(r_2 - r_1)(r_2^2 - r_1^2)^2} = 7.5 \times 10^7 fQ^2 \qquad \text{(A-3)}$$

Entrance and exit head losses for flow through the annular space are given by

$$h_{fi} = 1.5 \times 10^5 Q^2$$
$$h_{fo} = 3.0 \times 10^5 Q^2$$

A.2 Frictional Head Loss in the Upper Sub

From the annular space in the probe carrier, water flows up through three small circular holes in the upper sub and into the shut-in tool. In this section, frictional head losses into, through, and out of these holes in the upper sub are estimated.

Frictional head loss for incompressible, uniform, turbulent flow in a circular pipe or hole of constant diameter is given by the Darcy-Weisbach equation (Robertson and Crowe, 1980),

$$h_f = \frac{f\, L_{US}\, V^2}{D\ 2\ g} \qquad \text{(A-4)}$$

where: L_{US} = length of holes in upper sub [L]
D = internal diameter of pipe or hole [L]
V = velocity through holes [Lt^{-1}]
$= Q/A_T$

In this case, A_T is the total cross-sectional area of the three holes, so the total head losses are given by

$$h_f = \frac{8\, f\, L_{US}\, Q^2}{3\pi^2 D^5 g}$$
$$= 3.6 \times 10^7\, fQ^2 \qquad \text{(A-5)}$$
$$h_{fi} = 1.7 \times 10^6\, Q^2$$
$$h_{fo} = 3.3 \times 10^6\, Q^2$$

A.3 Frictional Head Loss Through the Shut-In Tool

Water flows from the upper sub up into the shut-in tool. In the shut-in tool, the water flows through six rectangular, radially aligned slits, then up into the riser pipe. In this section, frictional head losses into, through, and out of these six slits in the shut-in tool are estimated.

Frictional losses through six slits can be estimated using equation (A-1) with $A_T = 6hw$ and $P = 12\,(h+w)$ where h = height of slit [L] and w = width of slit [L].

Inlet and outlet head losses are given by equation (A-2). Therefore, total frictional head losses in the shut-in tool are given by

$$h_f = \frac{f\ L_{SI}(h+w)\ Q^2}{24\ gh^3w^3} \qquad \text{(A-6)}$$

$$= 6.1 \times 10^4 \, fQ^2$$

$$h_{fi} = 5.3 \times 10^4 \, Q^2$$

$$h_{fo} = 1.1 \times 10^5 \, Q^2$$

A.4 Frictional Head Loss through the Riser Pipe

From the shut-in tool, water flows up into the riser pipe and to the surface. In this section, frictional losses through the riser pipe are estimated.

Frictional losses through the riser pipe are given by equation (A-1). For this case, the total frictional head loss is

$$h_f = \frac{8 \, f \, L_{RP}}{\pi^2 D_{RP}^5 g} Q^2 \qquad \text{(A-7)}$$

$$= 4.8 \times 10^8 \, fQ^2$$